Sini decoction ameliorates sepsis-induced acute lung injury via regulating ACE2-Ang (1-7)-Mas axis and inhibiting the MAPK signaling pathway

Qiuhua Chen[a,1], Junjun Liu[b,1], Wanqiu Wang[b], Suzi Liu[b], Xiaoting Yang[b], Mingqi Chen[a], Lu Cheng[a], Jun Lu[a], Tao Guo[a,*], Fengjie Huang[b,*]

[a] Affiliated Hospital of Nanjing University of Chinese Medicine, Nanjing, China
[b] School of Life Sciences and Technology, China Pharmaceutical University, Nanjing, China

ABSTRACT

Sepsis, as life-threatening organ dysfunction caused by a dysregulated host response to infection, is characterized by the extensive release of cytokines and other mediators. Sini decoction (SND), a traditional Chinese prescription medicine, has been used clinically for the treatment of sepsis. But its explicit mechanism of action is still unclear.

The present study aims to evaluate the potential protective effects of SND on sepsis-induced acute lung injury (ALI). After SND intervention, the lung tissues of each experimental group were collected. H&E sections were used to observe the pathological changes of lung tissue, and alveolar lavage fluid was collected to detect the infiltration of inflammatory cells. Level of inflammatory factors in lung tissue were analyzed by qRT-PCR. The change of Renin angiotensin system (RAS), as well as downstream MAPK/NF-κB signaling pathways were measured by Western blot. For in vitro experiments, human umbilical vein endothelial cells (HUVECs) were pretreated with lipopolysaccharide (LPS) and treated with SND. Subsequently, the expression levels of RAS and MAPK/NF-κB signaling pathways were measured by Western blot.

In vivo, we found that SND significantly attenuated sepsis-induced pathological injury in the lung. SND also inhibited LPS-mediated inflammatory cell infiltration, the expression of pro-apoptotic proteins and the production of IL-6, IL-1β, TNF-α and MCP-1. In vitro, experiments using a co-culture of HUVECs with SND showed that there was a decrease in pro-apoptotic protein and pro-inflammatory mediator. In this research, we also found that SND protective action could be attributed to the regulation of renin-angiotensin system (RAS). MAPKs and NF-κB pathways.

To conclude, our study demonstrated that SND ameliorates sepsis-induced-ALI via regulating ACE2-Ang (1-7)-Mas axis and inhibiting the MAPK signaling pathway.

1. Introduction

Sepsis, as life-threatening organ dysfunction caused by a dysregulated host response to infection, is a major public health concern, accounting for more than $20 billon (5.2%) of total US hospital costs in 2011 [1]. It is characterized by systemic activation of the host inflammatory response and multiple organ dysfunction syndromes [2]. The lung is considered as the major vital organ that tends to be damaged by sepsis, in which ALI frequently occur [3]. Acute respiratory distress syndrome (ARDS), which is one of the most severe subtypes of ALI, is the primary cause of death from sepsis [3,4]. A previous study found that increasing permeability of vascular endothelial results in

pulmonary edema in patients with sepsis [5]. The disruption of alveolar barrier lead to the accumulation of proteins and macrophages, neutrophils in the alveolar space [6,7].

SND, a famous traditional Chinese medicine prescription, is consisted of three different Chinese herbs: Aconite, Liquorice and Ginger Rhizome. Aconite is the primary pharmacological component of SND. However, it exhibits strong toxicity due to aconitine alkaloids. Under the intervention of two other herbs, the toxicity can be greatly reduced. Studies have shown that proper aconitine alkaloids seems to be necessary for clinical therapeutics [8]. SND was first mentioned in the "Treatise on Febrile Diseases" of Zhongjing Zhang in the Han Dynasty. Which is a classic prescription for treating kidney yang deficiency and

reducing yin deficiency and cold syndrome. Clinically, Sini Decoction is often used to treat patients with sepsis and can significantly alleviate the condition [9,10]. Previous research found that SND significantly decreased inflammatory responses in myocardial infarction rats [11]. In CLP septic rats, SND protects against injury induced by sepsis through downregulation of adrenal TLR4 expression [12]. In our previous research, we found that SND restrained the expression level of IL-6, IL-1β and TNF-α, apoptosis and oxidative stress in mice ALI model [13]. These studies suggest that SND might be a potential therapy in sepsis-induced ALI.

The RAS is a complex hormone system and classically known as a regulator of blood pressure [14]. Related researches reported the disturbance of tissue intrinsic RAS is involved in the pathogenesis of ALI [15,16]. Angiotensin-converting enzyme 2 (ACE2), a bioactive enzyme of the RAS, plays a key role in the initiation and the maintenance of lung injury [17]. ACE2 reduces the expression of angiotensin II through catalyzing the conversion of Ang II to angiotensin-(1-7) (Ang-(1-7)), which restrains the vasoconstrictive, inflammatory, apoptosis and oxidation stress induced by Ang II [18,19]. Research showed recombinant ACE2 significantly reduced the cell apoptosis and the expression levels of inflammatory cytokines in LPS-induced pulmonary microvascular endothelial cells by inhibiting c-Jun N-terminal kinase (JNK) and NF-κB pathways [20]. Our previous studies demonstrated that SND could protect against inflammatory factor release, apoptosis and oxidative stress in *E.coli*–induced ALI via modulating ACE-AngII-AT1R and ACE2-Ang-(1-7)-Mas axis [13]. However, the downstream molecular detailed mechanism of RAS is not very clear.

Mitogen-activated protein kinases (MAPKs), a family of serine-threonine protein kinases, is consisted of stress-activated JNK, p38 and growth factor-regulated ERK1/2 and play vital roles in the regulation of certain cellular properties [21,22]. Previous studies have reported that MAPKs signaling pathway was activated in ALI, and inhibiting MAPKs can effectively alleviate the disease [23,24]. Captopril, ACE inhibitor, had protective effects on LPS-induced lung injury and the cytotoxicity of PMVECs via regulating the balance of ACE and ACE2 expression and inhibiting the activation of MAPKs [25]. The recent discovery indicated that up-regulation of the ACE2/Ang-(1-7)/Mas axis protected against pulmonary fibrosis by inhibiting the MAPK/NF-kB pathway [26]. NF-κB, which can be activated by MAPKs, regulates transcription of inflammatory factors [27]. In ALI, activated NF-κB promotes transcription of inflammatory factors and exacerbates disease progression [28].

Hence, our study aimed to investigate the mechanism by which SND protects against sepsis-induced ALI in vivo and in vitro. We discovered that SND protected against sepsis-induced ALI by upregulating the ACE2-Ang (1-7)-Mas axis and inhibiting the MAPK signaling pathway.

2. Materials and methods

2.1. Drug and reagents

Aconite (*Aconitum carmichaeli Debx*, root), Liquorice (*Glycyrrhiza uralensis Fisch*, root and rhizome), and Ginger Rhizome (*Zingiber officinale Roscoe*, rhizome) were purchased from Jiangsu Province Hospital of TCM. The ratio of these three herbs is 10:15:12. The preparation method of SND according to the literature description [13]. LPS (*Escherichia coli*, O55: B5) was purchased from Sigma-Aldrich (St. Louis, MO, USA). D-Ala7)-Angiotensin I/II (1-7) trifluoroacetate salt (A-779), a specific antagonist of G-protein coupled receptor (Mas receptor), was obtained from Bachem AG (Hauptstrasse, Bubendorf, Switzerland).

2.2. MTT assay of cell viability

The effect of SND on HUVEC cells viability was measured using the standard MTT assay as previously described [29]. HUVEC cells were plated at a density of 2×10^4 cells per well in a 96-well plate and incubated at 37 °C for 12 h. The cells were treated with various concentrations of SND (6.2, 12.5, 25 or 50 mg/mL) for 24 h. Cells were incubated with MTT solution for 4 h. The supernatant in the wells was carefully discarded, 150 μL of DMSO was added to each well and shaken for 20 min in the dark. Absorbance was measured at 570 nm (reference 630 nm) using a microplate reader (Multiscan FC, Thermo-Fisher Scientific, Rockford, IL, USA).

2.3. Cell culture and treatments

HUVECs were purchased from China National Type Culture Collection Cell Bank and maintained in RPMI-1640 supplemented with 5% fetal bovine serum (Wisent, China) at 37 °C, under a 5.0% CO_2 atmosphere. HUVECs were divided into the following four groups: (1) control group: HUVECs were treated with a cell culture medium. (2) LPS group (LPS): HUVECs were stimulated by LPS (1 μg/mL) for 24 h. (3) SND + LPS group: HUVECs were stimulated with LPS for 1 h and treated with SND at 6.2, 12.5, 25 or 50 mg/mL for 24 h. (4) A779 group (A779): After HUVEC cells were stimulated with LPS for 30 min, the A779 (100 μmoL/L) was added to the culture medium for 30 min. Then HUVEC cells were treated with SND at 25 mg/mL for 24 h.

2.4. Experimental mouse models

All animal procedures were approved by the China pharmaceutical University Experimental Animal Ethics Committee. Male adult ICR mice, weighing 25 ± 2 g, were obtained from Yangzhou University. The animals were kept at an environmentally controlled room temperature (25 ± 2 °C) in a light/dark cycle of 12 h, with free access to food and water. Induction of sepsis in a mouse model by intraperitoneal injection of LPS (8 mg/kg). Briefly, mice were divided into four groups (12 mice in each group): control group, LPS group, SND group and SND + A779 group. The control group received equal volumes of PBS. In SND group, after Intraperitoneal injection of LPS for 2 h, mice were treated by SND (5 g/kg, 400 μL) through oral administration twice daily (9 a.m. and 6 pm). In SND + A779 group, after intratracheal infusion of LPS for 1 hour, mice were treated by A779 (500 μg/kg/day, 100 μL, ip). Then the mice were treated by SND through oral administration twice daily (9 a.m. and 6 pm).

2.5. Animal sample collection

Following the LPS challenge after 24 h, the mice were anesthetized with pentobarbital sodium (50 mg/kg). BALF, lung tissue and blood were collected for further analyses; BALF and lung homogenate were obtained from three animals in each group, and the lungs for histological examination and lung wet/dry weight ratio were obtained from the remaining three animals in each group.

2.6. Collection of bronchoalveolar lavage fluid (BALF)

After the mouse was sacrificed, the skin was cut open to expose the trachea. Then we injected 0.3 mL PBS into the lung through a tracheal cannula and aspirated the liquid for three times to obtain BALF. The BALF was centrifuged at 3000 rpm for 10 min at 4 °C. The resuspended cells were stained with Giemsa stain, and then neutrophil and macrophages were counted under a microscope. The total cells were counted by blood counting chamber, and the supernatant was harvested for total protein analysis using the BCA protein assay kit (Beyotime, China).

2.7. Lung wet/dry (W/D) ratio

To assess oedema, the left lung was harvested immediately and then the wet weight was weighed using an electronic balance. The lung was then placed in a thermostatic oven at 68 °C for 48 h, the dry weight recorded and the lung wet-to-dry weight ratio was determined.

2.8. Histologic examination

Three sections were cut from each group. H&E staining was performed to assess the morphologic changes in injured lung tissue. Briefly, the lung tissues were fixed in 10% formalin, paraffin-embedded and then sectioned into 5 μm slices (Servicebio technology). The sections were photographed in 5 random fields under a microscope. The degrees of lung injury were assessed according to the literature description [13]. The expression of ACE2 in lung tissues was detected by immunohistochemistry staining. The paraffin-embedded lung tissue sections were deparaffinized in xylene, dehydrated by graded concentrations of alcohol, heated in retrieval solution in a microwave at low power for 10 min, and then incubated with 5% BSA (AR0004, Boster, China) for 60 min. The slides were then incubated with ACE2 primary antibody at 4 °C overnight. After washing with PBS, biotin-labeled secondary antibody was added. Finally, slides were visualized by DAB horseradish peroxidase colour development Kit (Beyotime, China). Under 400× magnification (Motic china group co, ltd).

2.9. qRT-PCR

Total RNA was extracted from freshly isolated lung tissues and HUVEC cells using Trizol (CW0580 CWBIO, China) following the kit's instructions. Isolated RNA was reverse-transcribed into cDNA with HiFiScript cDNA Synthesis Kit (CW2569 CWBIO, China). Quantitative real-time PCR was operated with QuantStudio 7 Flex Real-Time PCR System (ThermoFisher) and the AceQ Universal SYBR qPCR Master mix (P612-01, VAZYME, China). The mRNA levels of IL-6, IL-1β, TNF-α, MCP-1 and GAPDH in lung tissues and HUVEC cells were examined by qRT-PCR. The mRNA expression levels were displayed as fold change over that of the internal-control GAPDH. Primer sequences of qRT-PCR test (Table 1).

2.10. Western blots

For western blot analysis, homogenized lung tissues and treated HUVEC cells were lysed in RIPA lysis buffer (Beyotime, China) with protease and phosphatase inhibitors for 2 h at 4 °C, followed by centrifugation at 12,000 rpm for 10 min at 4 °C. The supernatants were collected, and BCA method (P0010S, Beyotime, China) was used to determine protein concentration. Protein samples were separated by 8–10% SDS-PAGE, and were transferred to a PVDF membrane. The membrane was blocked in 5% skim milk at room temperature for 90 min, blotted with each primary antibody overnight at 4 °C and the corresponding secondary antibody (1:10,000) at room temperature for 2 h. ACE (ET1705-36 1:1000 HuaBio China), ACE2 (ET1611-58 1:1000 HuaBio China), ATIR (Bs-0630R 1:1000 Bioss), MAS1 (Bs-5925R 1:1000 Bioss), p38 (ET1602-26 1:1000 HuaBio China), p-p38 (WLp2031 1:500 Wanleibio), Jnk (WL01295 1:500 Wanleibio), p-Jnk (WL03507 1:500 Wanleibio), ERK1/2 (ET1601-29 1:1000 HuaBio China), p- ERK1/2 (WLp1512 1:500 Wanleibio), IκB (WL0053 1:500

Wanleibio), p-IκB (WL02495 1:500 Wanleibio), p65 (WL01980 1:500 Wanleibio), p-p65 (WL02169 1:500 Wanleibio), Occludin (R1510-33 1:1000 HuaBio China), VE Cadherin (Bs-4310R 1:1000 Bioss), Caspase 3 (ER30804 1:1000 HuaBio China), Caspase 9 (ET1603-27 1:1000 HuaBio China), Bcl-2 (WL01556 1:500 Wanleibio), Bax (ER0907 1:1000 HuaBio China), PARP (WL0326 1:500 Wanleibio), GAPDH (AB0037 1:3000 Abways Technology). Finally, proteins were visualized with an enhanced chemiluminescence detection kit (Tanon, China) and analyzed with Gel-pro Analyzer.

2.11. Measurements of MDA, SOD contents

The levels of MDA (A003-1, Nanjing Jiancheng, China), and SOD (A001-3, Nanjing Jiancheng, China) in serum were determined by commercially available test kits according to the manufacturer's kit protocols.

2.12. Enzyme-linked immunosorbent assay

Applying a commercially available mouse ELISA kits, the levels of AngII (MM-0754M2, Meimian, China) and Ang-(1-7) (MM-0207M2 Meimian, China) in serum were detected. The absorbance was read at 450 nm with a microplate reader.

2.13. Statistical analysis

All data were represented as mean ± standard error of the mean (SEM). The statistical analysis for this study was analyzed using Student's *t*-test between two groups and one-way analysis of variance (ANOVA) for multiple groups. Data was analyzed using Graph Pad prism software (version5.0).

3. Results

3.1. SND treatment attenuated sepsis-induced ALI in mice

The severity of sepsis-induced ALI was determined by histological analysis and the BALF method. The pathological changes in lungs were detected by H&E staining. As shown in Fig. 1(A, B), mice treated with LPS displayed severe inflammatory cell accumulations and destruction of alveolar histological structure compared with control group mice. Furthermore, the LPS group showed severe alveolar edema fluid accumulation and alveolar capillary congestion. After treatment with SND, the pathology of lung injury was markedly decreased. Similarly, we determined the protein concentration in BALF and the lung W/D ratio. As shown in Fig. 1(C, D), compared with the control group, protein concentration in BALF and the lung W/D ratio increased dramatically under LPS stimulation. However, these were relieved dramatically by SND treatment. To further evaluate the protective effect of SND on lung tissues, the number of inflammatory cells in BALF was quantified. As shown in Fig. 1(E−G), the number of total cells, neutrophils and

Table 1
Primer sequences of qRT-PCR test.

| Name	Species	Forward Primer (5'-3')	Reverse primer (5'-3')
IL-6	Mouse	CTGCAAGAGACTTCCATCCAG	AGTGGTATAGACAGGTCTGTTGG
	Human	ACCTTCCAAAGATGGCTGAA	GCTCTGGCTTGTTCCTCACT
IL-1β	Mouse	GAAATGCCACCTTTGACAGTG	TGGATGCTCTCATCAGGACAG
	Human Mouse	AGTTGCCTTCTTGGGACTGA	TCCACGATTTCCCAGAGAAC
TNF-α	Human	CCTGTAGCCCACGTCGTAG	GGGAGTAGACAAGGTACAACCC
	Mouse	CCTCTCTCTAATCAGCCCTCTG	GAGGACCTGGGAGTAGATGAG
MCP-1	Human	TTAAAAACCTGGATCGGAACCAA	GCATTAGCTTCAGATTTACGGGT
	Mouse	GCTCATAGCAGCCACCTTCATTC	GTCTTCGGAGTTTGGGTTTGC
GAPDH	Human	CTCTCTGCTCCTCCTGTTCGACAG	GTGGAATCATATTGGAACATGT
		GACAAGCTTCCCGTTCTCAG	GACAAGCTTCCCGTTCTCAG
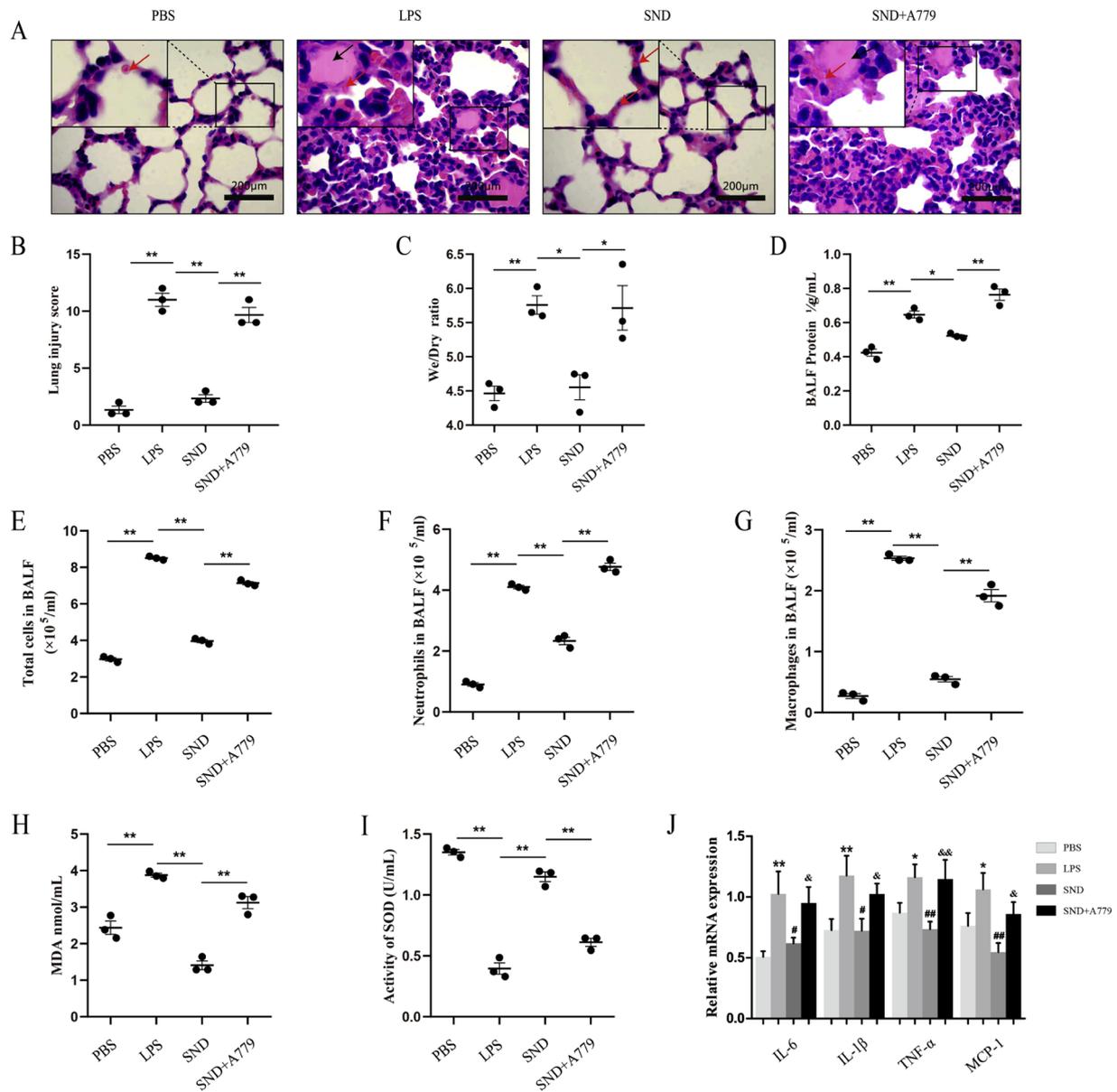
Fig. 1. SND treatment attenuates sepsis-induced ALI in mice. (A). Lung tissues from each experimental group were obtained at 24 h after LPS administration and processed for histological evaluation by H&E staining. Red arrow: alveolar capillary. Black arrow: edema fluid. (magnification 400x). (B). Pathological lung injury scores. (C). The effects of SND on pulmonary edema were assessed by W/D weight ratios. (D). Total protein concentration in BALF was measured by a BCA method. The number of different inflammatory cells in BALF: (E). Total cells. (F). neutrophils. (G). macrophages. (H). The levels of SOD activity in serum. (I). MDA level in serum. (J). The levels of proinflammatory cytokines (IL-6, IL-1β, TNF-α, and MCP-1) in lung tissues were detected by qRT-PCR ($^*p < 0.05$ vs. PBS group, $^{**}p < 0.01$ vs. PBS group, $^#p < 0.05$ vs. LPS group, $^{##}p < 0.01$ vs. LPS group, $^&p < 0.05$ vs. SND group, $^{&&}p < 0.01$ vs. SND group). Data were represented as the mean ± SEM of three independent experiments. (n = 3 per group, $^*p < 0.05$, $^{**}p < 0.01$).

macrophages in BALF were increased remarkably in LPS group compared to control group, which could be significantly decreased by SND treatment. We also measured the level of oxidative stress, the results showed that LPS could increase the level of MDA and significantly decrease activity of SOD in serum (Fig. 1H, I). As expected, SND significantly improved the changes caused by LPS. Pro-inflammatory mediator levels in tissues were detected by qRT-PCR. The results were displayed in Fig. 1J, SND greatly inhibited LPS-induced IL-6, IL-1β, TNF-α and MCP-1 mRNA levels in lung tissues. Interestingly, the therapeutic effect of SND will be reversed in the SND + A779 group (Fig. 1A–J). It suggested that the improvement of SND on sepsis-induced ALI was associated with RAS.

3.2. SND treatment ameliorated the apoptosis on sepsis-induced ALI

We moved on to determine the effect of SND inhibition on the expression levels of apoptotic proteins. Bcl-2 family members, a vital role in mitochondrial permeability, are mainly classified into the pro-apoptotic Bax and anti-apoptotic Bcl-2 proteins that control activation of caspase cascade [30]. Western blot results showed that the expression of Bax was visibly upregulated, and Bcl-2 was decreased under LPS stimulation compared with the control (Fig. 2A–C). Treatment of septic mice with SND produced a significant increase in expression of Bcl-2 and decrease in expression of Bax. Caspase proteins play an important role in the execution phase of apoptotic progress. As shown in Fig. 2(D–G), SND could significantly inhibit the activation of caspase 9, caspase 3 and PARP in sepsis-induced ALI. The results suggested that
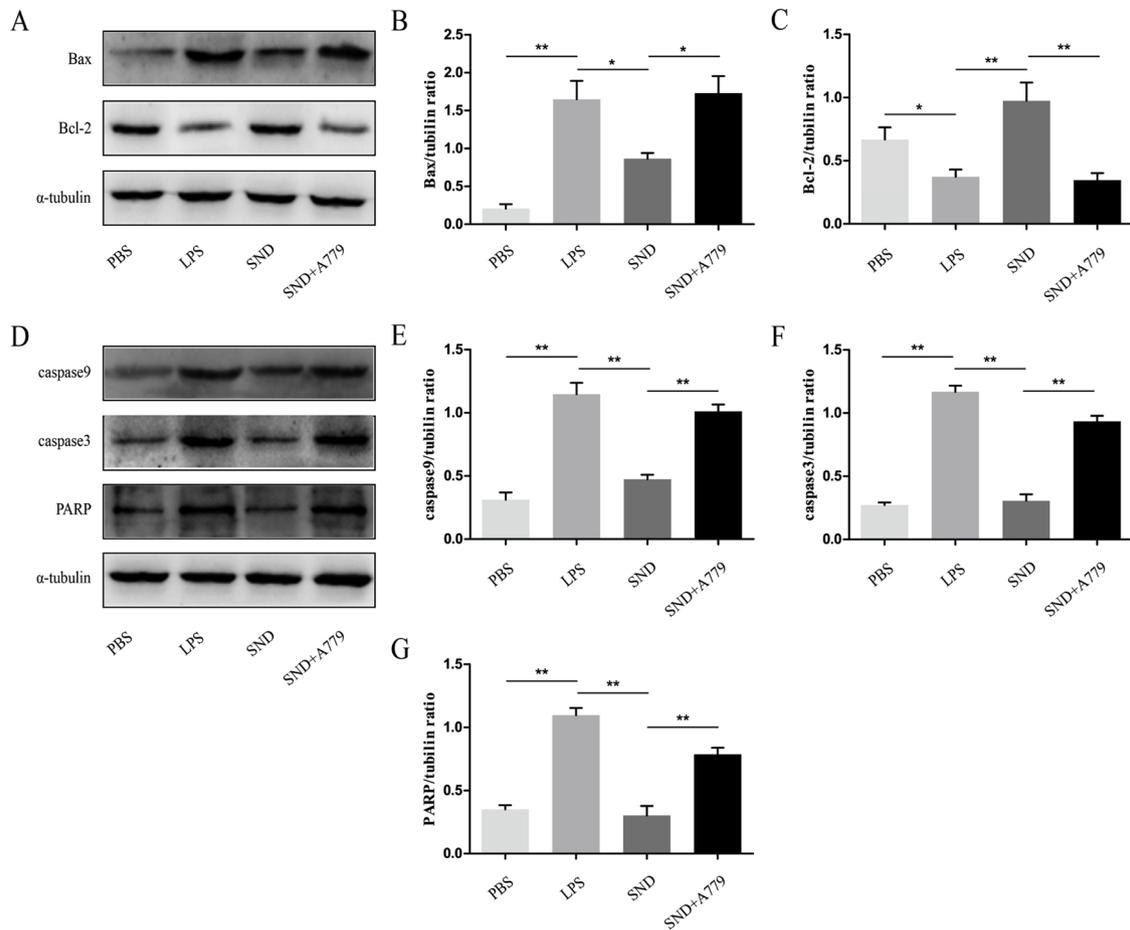
Fig. 2. SND treatment ameliorates the apoptosis on sepsis-induced ALI. After LPS administration for 24 h, the levels of Apoptotic proteins in lung tissues were measured by western blot. (A–C). Expression levels of Bax and Bcl-2 in sepsis-induced ALI. (D–G). Expression levels of caspase 3, caspase 9 and PARP in sepsis-induced ALI. Data were represented as the mean ± SEM of three independent experiments. (n = 3 per group, $^*p < 0.05$, $^{**}p < 0.01$).

SND had a significant inhibitory effect on mitochondria-mediated apoptosis pathway by modulating the activation of the caspase cascade. Similarly, the effect of SND on apoptotic proteins was removed after exogenous A779 interference (Fig. 2A–G).

3.3. SND mediated the inhibitory effect of ACE2/Ang-(1–7) on sepsis-induced ALI in mice

To further explore the protective mechanism of SND underlying sepsis-induced ALI, we evaluated the effect of SND on renin-angiotensin system (RAS). ACE and AT1R expression were increased in the LPS groups, but decreased in the SND group (Fig. 3A–C). The levels of ACE2 and MasR were detected by Western blot (Fig. 3D–F). The data suggested that the contents of ACE2 and MasR in the LPS group were obviously decreased compared to the control group, and the levels of ACE2 and MasR in SND-treated mice were obviously higher than LPS group. According to the immunohistochemical staining, SND also increased the ACE2 expression in the lung tissue. In addition, the concentrations of Ang II and Ang-(1-7) in serum were measured via ELISA. As shown in Fig. 3(H, I). LPS could noticeably increase the concentration of Ang II in serum, but had no significant effect on Ang-(1-7). However, the concentration of Ang-(1-7) was obviously increased and the concentration of Ang II was conversely decreased in SND group. As expected, A779 could reverse the phenomenon that effect of SND on RAS. All these results suggested that SND could upregulated ACE2/Ang-(1–7) and down-regulate ACE/AT1R axis.

3.4. SND downregulated MAPK pathways under in vitro

The MAPK activation level was examined in lung tissue by Western blotting analysis. As shown in Fig. 4(A–D), LPS substantially induced the phosphorylation of p38, ERK1/2 and Jnk, when the mice were treated with SND, LPS-induced p38, ERK1/2 and Jnk activation were blocked. Furthermore, we found that pre-treatment of SND treated mice with A779 completely restored phosphorylation of p38, ERK1/2 and Jnk, which suggested that SND inhibited MAPK signaling pathways associated with ACE2/ Ang-(1-7)/MasR axis activation. NF-κB is activated rapidly in response to a wide range of stimuli, including pathogens, stress signals, and proinflammatory cytokines. As shown in Fig. 4(E–G), the phosphorylation of p65 in LPS-treated mice was dramatically inhibited by SND. Furthermore, IκB was markedly degraded after treatment with LPS, whereas treatment with SND prevented this degradation. These data suggested that SND may block the activation of NF-κB signaling in sepsis-induced ALI in mice.

3.5. SND treatment ameliorated the pro-inflammatory Cytokines and Apoptosis proteins induced by LPS in HUVECs

The MTT assay was used to detect whether SND was cytotoxic to HUVECs. When the concentration of SND was in the range of 0–12.5 mg/mL, it was not toxic to cells. However, at a concentration of 25 mg/mL, SND showed significant cytotoxicity (Fig. 5A). To illustrate the effects of SND on endothelial permeability-associated proteins, we examined endothelial Occludin and VE-cadherin expression. The results showed that proteins expression of Occludin and VE-cadherin were
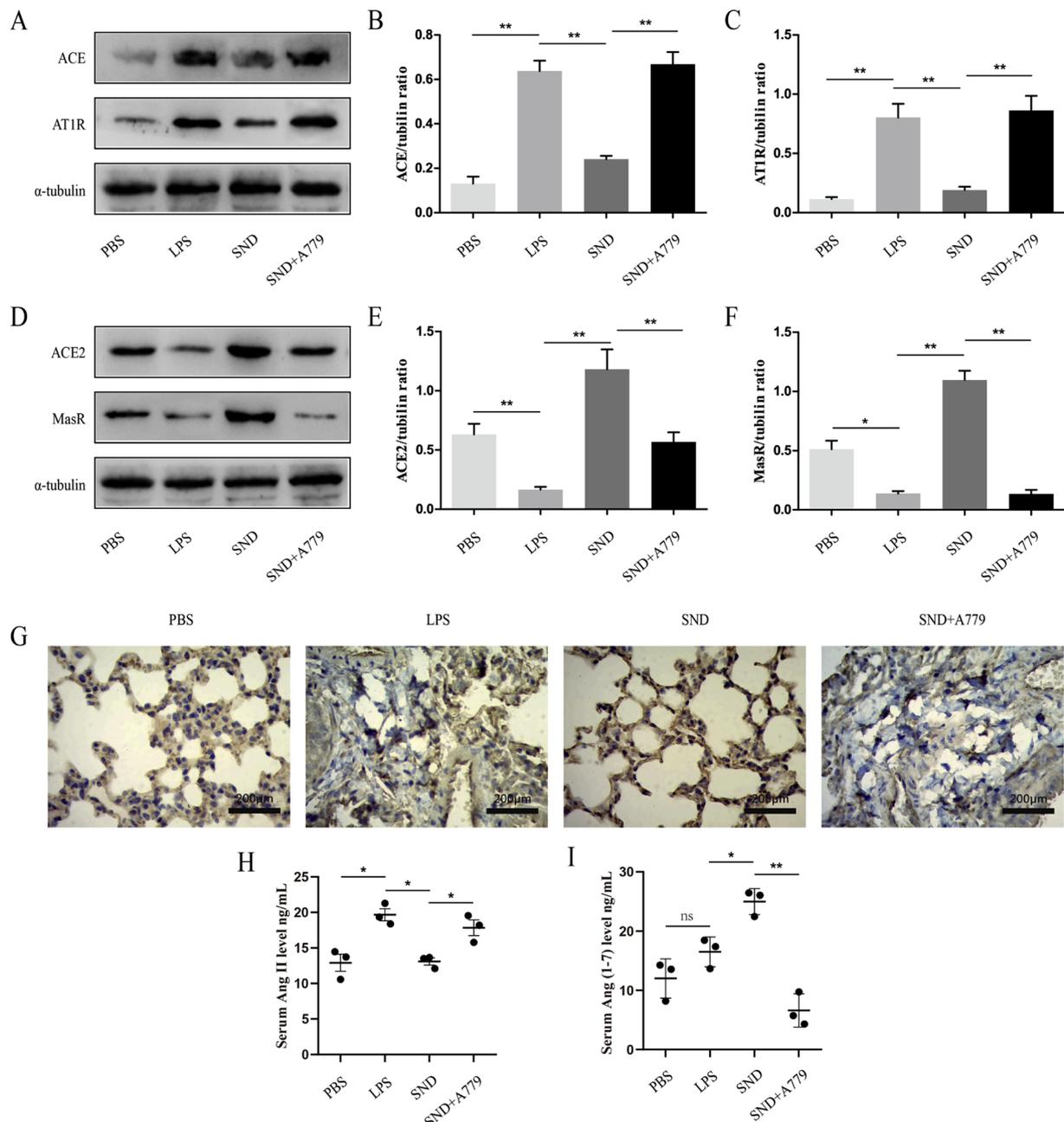
Fig. 3. SND mediated the inhibitory effect of ACE2/Ang-(1–7) on sepsis-induced ALI in mice. (A–C). Expression levels of ACE and AT1R in sepsis-induced ALI. (D–F). Expression levels of ACE2 and MasR in sepsis-induced ALI. (G). Expression levels of ACE2 in the lung tissue was measured by immunohistochemical staining. (H–I). After LPS administration for 24 h, the levels of Ang II and Ang-(1-7) in serum were detected by ELISA. Data were represented as the mean ± SEM of three independent experiments. (n = 3 per group, *p < 0.05, **p < 0.01).

noticeably reduced after LPS stimulation. However, SND could promote the expression of Occludin and VE-cadherin in a dose-dependent manner. When the concentration of SND was 25 mg/mL, the expression of Occludin and VE-cadherin reached the highest (Fig. 5B–D). In addition, we had evaluated the effects of SND on Occludin and VE-cadherin at different time points (Fig. 5G–J). The results showed that SND increased the expression of Occludin and VE-cadherin in a time-dependent manner and the effect of SND was most significant at 24 h. At the same time, we also evaluated the protein expression levels of ACE2 and ACE in HUVECs after SND treatment, the results showed that SND could abolish the effects of LPS in a time- and dose-dependent manner (Fig. 5B, G). Pro-inflammatory mediator levels in HUVECs were detected by qRT-PCR. As shown in Fig. 6A, treatment with LPS (1 μg/mL) for 24 h significantly induced the, IL-6, IL-1β, TNF-α and MCP-1 mRNA

expression. As expected, HUVECs were co-treated with SND (25 mg/mL) for 24 h effectively suppressed LPS-induced IL-6, IL-1β, TNF-α and MCP-1 mRNA expression. We further investigated the effect of SND on apoptotic proteins in HUVECs. As shown in Fig. 6(B–H), Our results showed that SND treatment downregulated expression of Bax, caspase 9, caspase 3 and PARP and upregulated expression of Bcl-2. However, the effect of SND was significantly blocked by A779.

3.6. SND regulated ACE2-Ang (1-7)-Mas/MAPK signaling pathway in HUVECs

Consistent with the results in mice, SND significantly activated ACE2-Ang (1-7)-Mas. As shown in Fig. 7(A–C), SND markedly enhanced the protein expression of ACE2 and MasR and prevented the LPS-
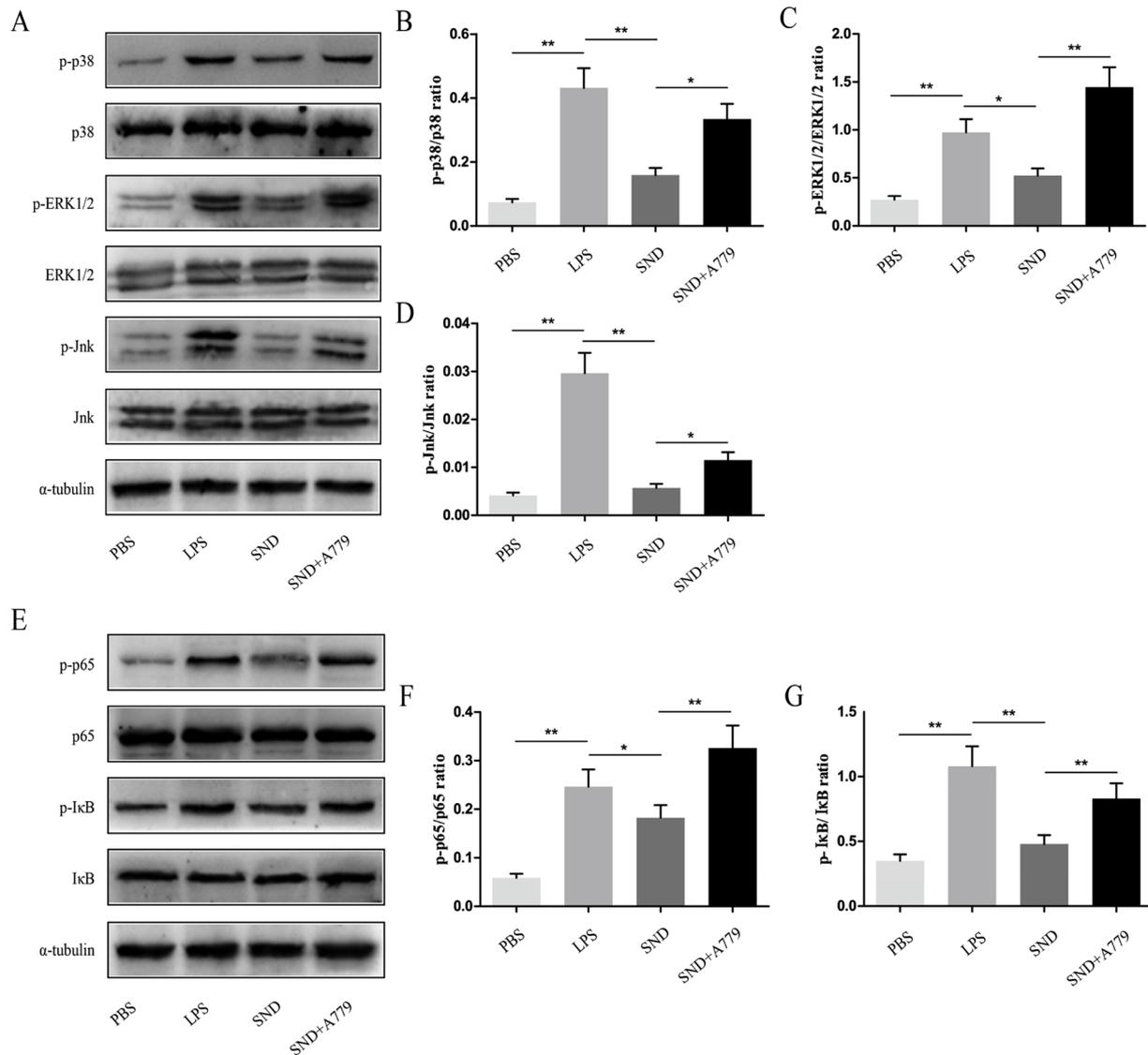
Fig. 4. SND downregulated MAPK pathways under In Vitro. (A–D): The MAPKs activation level were examined in lung tissue by Western blotting. (E–G): Expression and phosphorylation level of p65 and IκB proteins in sepsis-induced ALI. Data were represented as the mean ± SEM of three independent experiments. (n = 3 per group, $^*p < 0.05$, $^{**}p < 0.01$).

induced increase in ACE and AT1R (Fig. 7D,E). However, these effects were blocked by MasR antagonist A779. Similarly, we investigated whether SND influenced LPS-induced pro-inflammatory cytokine expression via regulation of the MAPK signaling pathway (Fig. 7F). Phosphorylation of p38, ERK and Jnk was significantly induced in LPS-stimulated HUVEC cells. As expected, SND inhibited LPS-induced phosphorylation of p38, ERK and Jnk. To further verify our results, we detected NF-κB signaling pathways by Western Blots. As shown in Fig. 8, the phosphorylation of p65 was dramatically inhibited by SND. Furthermore, SND markedly inhibited LPS-induced degradation of IκB. Taken together, these results indicated that SND protected HUVECs against injury caused by LPS.

4. Discussion

In this study, we evaluated the effect of SND therapy on a sepsis model and its potential mechanism of action in lung injury. Our study suggested that SND could improve the inflammation and apoptosis in sepsis-induced ALI via regulating ACE2-Ang (1-7)-Mas axis and inhibiting the MAPK and NF-κB signaling pathway.

Sepsis is defined by life-threatening organ dysfunction caused by a dysregulated host response to infection and endothelial dysfunction in response to the invading pathogenic agents [31]. This may develop into septic shock, leading to multiple organ dysfunction and possibly leading to death [32]. ALI and ARDS are common complications of sepsis [33]. Inflammation levels in the lungs were remarkably increased in the ALI model induced by intranasal instillation of LPS [23]. In another study, results indicated that MPO promoted the development of lung neutrophilia and indirectly influenced subsequent chemokine and cytokine production by other cell types in the lung [34]. As a traditional Chinese medicine, SND has been widely used in clinical diseases [35]. In our previous research, SND had a considerable effect on the treatment of ALI [13]. In this study, we demonstrated a possible mechanism of SND in the treatment of sepsis-induced ALI.

The analysis of pulmonary tissue and BALF revealed a beneficial effect of the SND. Our research demonstrated that sepsis mouse model evoked severe lung injury, which was characterized by severe inflammatory cell accumulation and destruction of alveolar histological structure. Lung W/D weight ratio was used as a measurement of increased capillary permeability and extravascular lung fluid [33]. Our
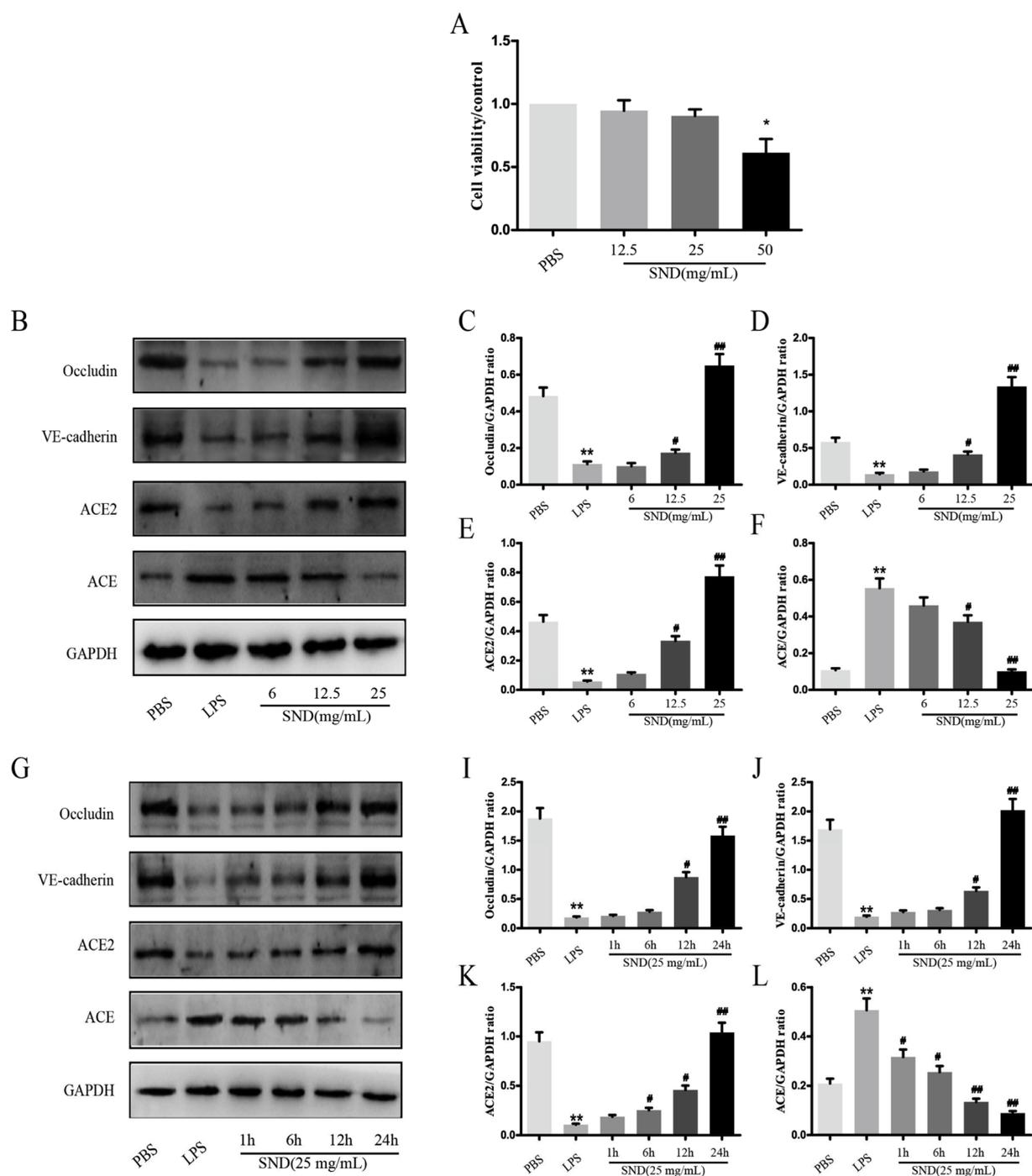
Fig. 5. SND treatment ameliorates the pro-inflammatory Cytokines and Apoptosis proteins induced by LPS in HUVECs. (A). HUVEC viability was assessed by MTT assay after treatment with different concentrations (12.5, 25, 50 mg/mL) of SND for 24 h. (B–F). HUVECs were treated with LPS (1 μg/mL) or PBS in the presence or absence of SND (6, 12.5, 25 mg/mL) for 24 h, then proteins expression level of Occludin, VE-cadherin, ACE2, and ACE was determined by. Western blotting. (G–L). HUVECs were treated with LPS (1 μg/mL) or PBS in the presence or absence of SND (25 mg/mL) for different time (1 h, 6 h, 12 h and 24 h), then proteins expression level of Occludin, VE-cadherin, ACE2, and ACE was determined by. Western blotting. Data were represented as the mean ± SEM of three independent experiments. (n = 3 per group, *p < 0.05 vs. PBS group, **p < 0.01 vs. PBS group, #p < 0.05 vs. LPS group, ##p < 0.01 vs. LPS group).

results showed SND had a positive therapeutic effect on lung structural lesions and W/D weight ratio. Another important feature of ALI is the increased permeability of pulmonary blood vessels and epithelium, leading to accumulation of protein-rich fluid in alveolar space [36]. Our results showed protein concentration was significantly increased after LPS treatment. In contrast, SND could restore protein levels to normal levels. MDA is a product of lipid peroxidation and serves as a marker of oxidative stress, and SOD exerts its antioxidant effect and may protect

against ALI [37]. ALI is invariably associated with highly expressed pro-inflammatory mediators including IL-6, IL-1β, TNF-α and MCP-1 [38]. These cytokines were measured by qRT-PCR in vivo and in vitro. Our analysis showed the elevated levels of IL-6, IL-1β, TNF-α and MCP-1 that were LPS-induced. However, they were dramatically inhibited by SND. Furthermore, our research found that it could downregulate the expression of Bax, caspase 9, caspase 3 and PARP and upregulate the expression of Bcl-2. This suggested that the protective effect of SND was
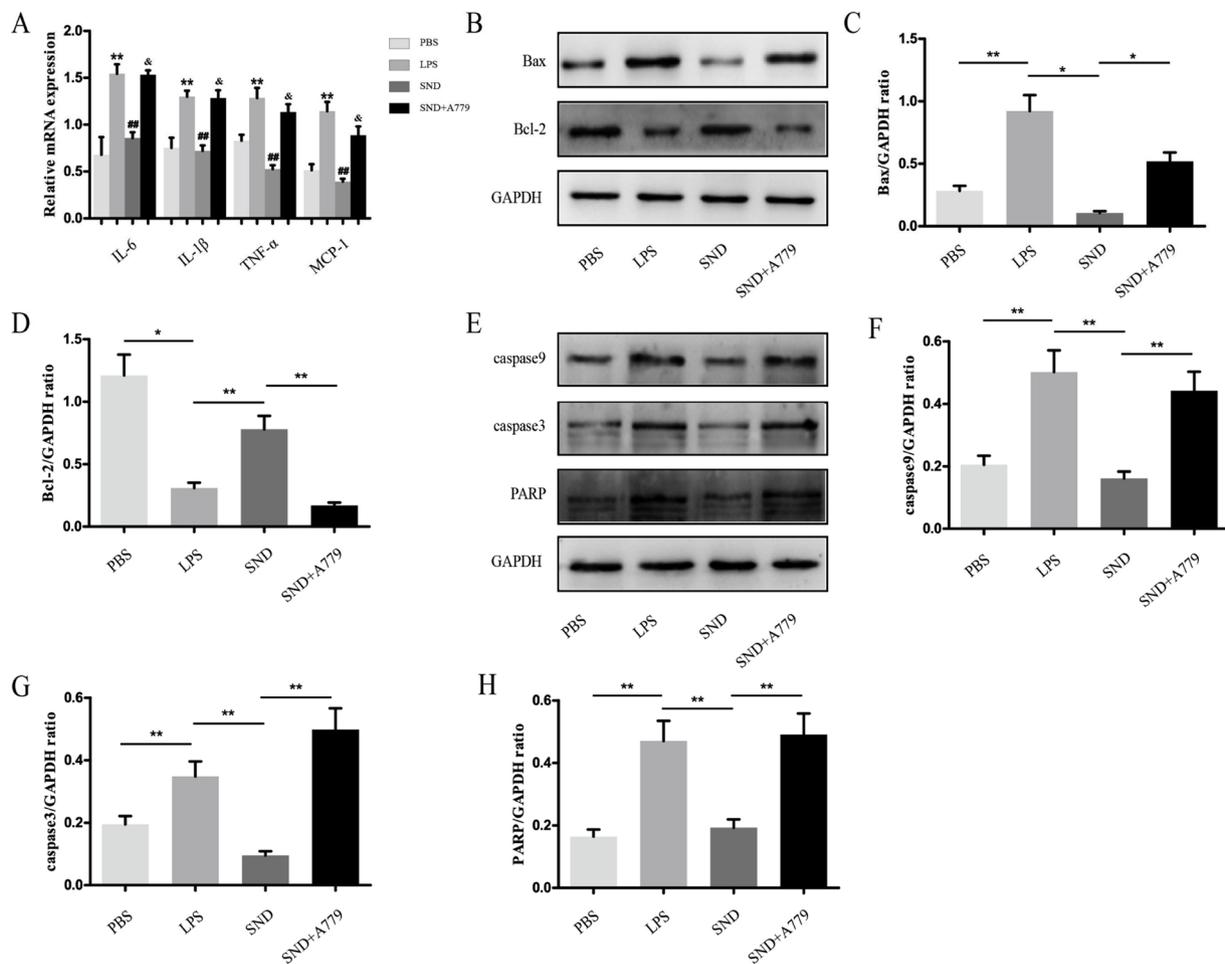
Fig. 6. SND treatment ameliorates the pro-inflammatory Cytokines and Apoptosis proteins induced by LPS in HUVECs. (A). HUVECs were treated with LPS (1 μg/mL) or PBS in the presence or absence of SND (25 mg/mL) for 24 h, then mRNA expression level of IL-6, IL-1β, TNF-α, and MCP-1 was determined by real-time PCR. (B–D). Expression levels of Bax and Bcl-2 in HUVECs. (E–H). Expression levels of caspase 3, caspase 9 and PARP HUVECs. Data were represented as the mean ± SEM of three independent experiments. (n = 3 per group, *p < 0.05, **p < 0.01).

associated with anti-inflammatory and anti-apoptosis.

RAS plays an important role in modulating blood pressure and cardiovascular remodeling [39,40]. Whereas, increasing evidence suggested that it was also important in regulating inflammatory responses. In the LPS-induced inflammation model, RAS contributed to upregulate ACE/Ang II/AT1R axis and downregulate ACE2/Ang (1-7)/Mas axis [41]. Accumulating evidence showed that RAS also played an important role in the occurrence and development of ALI [42]. Ang II acts as an important regulatory molecule in the RAS system and contributes to the inflammatory process by increasing the release of pro-inflammatory cytokines through the AT1R [43]. Recent studies have shown that ACE2 acts as a counter-regulator of ACE, activated the ACE2/Ang (1-7)/Mas axis significantly inhibits inflammatory responses [44]. In line with the previous study, our results showed that protein expression of ACE2 was raised by SND. The result was a significant decrease in expression of AT1R and Ang II, whereas Ang (1-7) was dramatically increased by SND. Furthermore, A779, a MasR antagonist, reversed these effects. These results suggested SND modulates the RAS in a positive manner. It reduced inflammatory cytokines, apoptotic proteins and improved LPS-induced damage in vivo and in vitro.

NF-κB is a multiprotein complex, which is involved in the early cellular defense responses of higher organisms and plays a key role in immune and inflammatory responses [45]. Excessive activation of the NF-κB aggravates inflammatory lesions in the lungs in ALI [46]. In this study, treatment with SND blocked the activation of the NF-κB and

degradation of IκB. Therefore, the production of various inflammatory factors in the lungs was reduced. SND also inhibited the activation of NF-kb signaling pathway in vitro. The mammalian family of mitogen-activated protein kinases includes p38, ERK1/2 and Jnk. Recent research has shown that MAPKs can activate NF-κB transcription [47]. To investigate whether the MAPKs pathway was associated with the protective eff ;ect of SND against sepsis-induced ALI, MAPKs pathway was detected by Western Blots in vivo and in vitro. Treatment with SND significantly attenuated the phosphorylation of p38, ERK and Jnk. Moreover, the Mas receptor antagonist abolished the attenuation effect of SND in sepsis-induced ALI. The results of our in vitro study also suggested that SND prevented HUVECs from LPS-induced apoptosis and inflammation by inhibiting MAPKs and NF-κB signaling pathway. These results suggested that RAS, MAPKs and NF-κB signaling pathway might be involved in the protective mechanism of SND in LPS-induced lung injury.

5. Conclusion

In conclusion, we have revealed an involvement of SND in the maintenance of sepsis-induced ALI. Our results have demonstrated that the protective effect of SND is directly related with upregulating the ACE2-Ang (1-7)-Mas axis and inhibiting the MAPK signaling pathway. The way that SND influences the host response is essential for an understanding in the search for repetition treatments for sepsis.
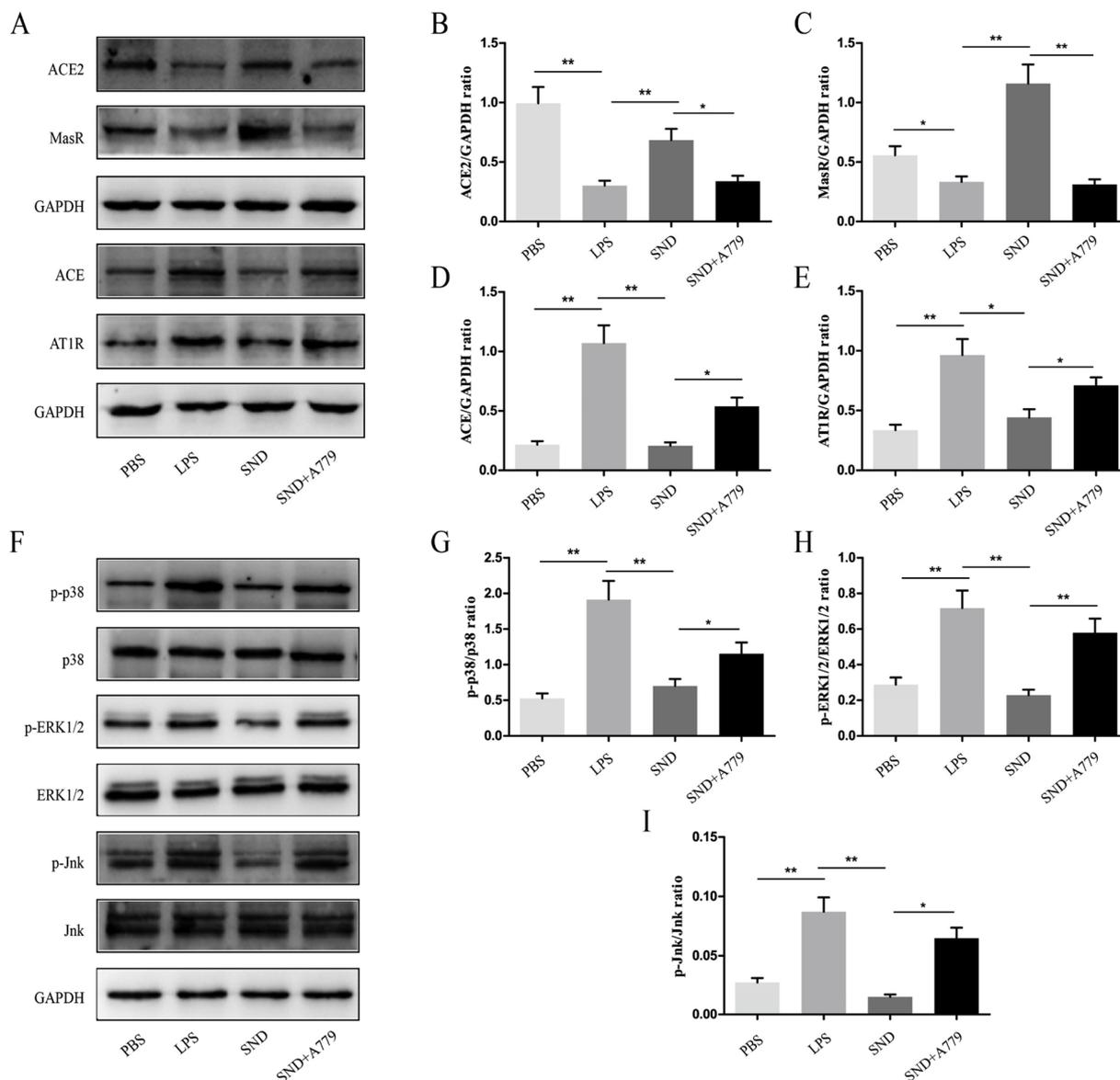
Fig. 7. SND regulated ACE2-Ang (1-7)-Mas/MAPK signaling pathway in HUVECs. HUVECs were treated with LPS (1 μg/mL) or PBS in the presence or absence of SND (25 mg/mL) for 24 h. (A–E). The expression levels of ACE, AT1R, ACE2 and MasR in HUVECs were measured by western blot. (F–I). The MAPKs activation level were examined in lung tissue by Western blotting. Data were represented as the mean ± SEM of three independent experiments. (n = 3 per group, *p < 0.05, **p < 0.01).
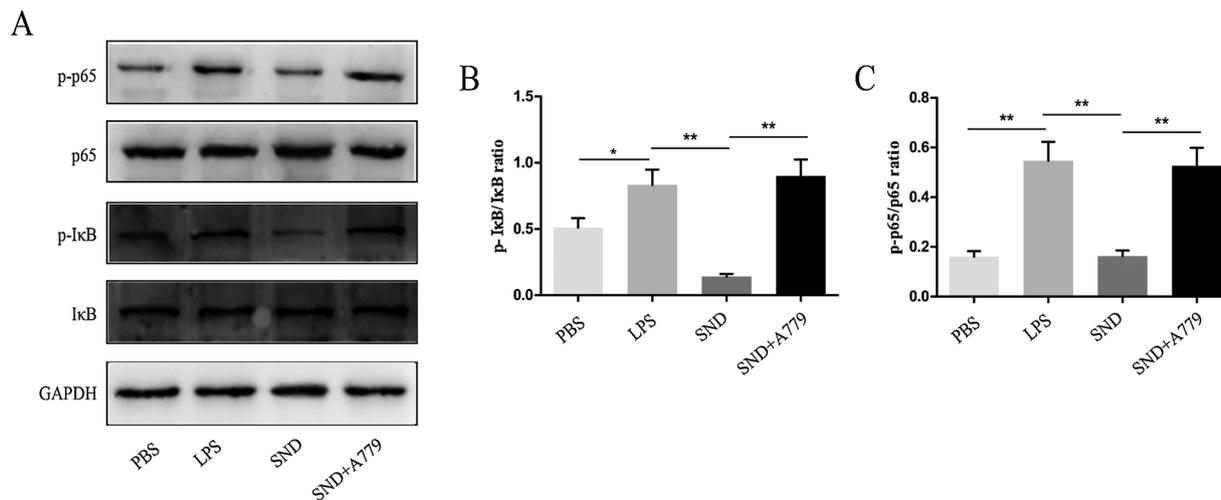

Fig. 8. SND regulated ACE2-Ang (1-7)-Mas/MAPK signaling pathway in HUVECs. HUVECs were treated with LPS (1 μg/mL) or PBS in the presence or absence of SND (25 mg/mL) for 24 h. Expression and phosphorylation level of p65 and IκB proteins in HUVECs. Data were represented as the mean ± SEM of three independent experiments. (n = 3 per group, *p < 0.05, **p < 0.01).

Authors' contributions

Fengjie Huang, Tao Guo, Qiuhua Chen and Junjun Liu conceived and designed the research. Qiuhua Chen and Junjun Liu performed most experiments and animal works. Wanqiu Wang, Suzi Liu, Xiaoting Yang, Mingqi Chen, Lu cheng, and Jun Lu assisted some experiments and result analysis. JL drafted and wrote the manuscript.

Conflicts of interest

The authors declare no conflict of interest.

Acknowledgments

References

[1] M. Singer, C.S. Deutschman, C.W. Seymour, M. Shankar-Hari, D. Annane, M. Bauer, et al., The third international consensus definitions for Sepsis and septic shock (Sepsis-3), JAMA 315 (2016) 801–810, https://doi.org/10.1001/jama.2016.0287.

[2] D.B. Knox, M.J. Lanspa, K.G. Kuttler, S.C. Brewer, S.M. Brown, Phenotypic clusters within sepsis-associated multiple organ dysfunction syndrome, Intensive Care Med. 41 (2015) 814–822, https://doi.org/10.1007/s00134-015-3764-7.

[3] M. Qian, Y. Lou, Y. Wang, M. Zhang, Q. Jiang, Y. Mo, et al., PICK1 deficiency exacerbates sepsis-associated acute lung injury and impairs glutathione synthesis via reduction of xCT, Free Radic. Biol. Med. 118 (2018) 23–34, https://doi.org/10.1016/j.freeradbiomed.2018.02.028.

[4] S. Bao, M.J. Liu, B. Lee, B. Besecker, J.P. Lai, D.C. Guttridge, et al., Zinc modulates the innate immune response in vivo to polymicrobial sepsis through regulation of NF-kappaB, Am. J. Physiol. Lung Cell Mol. Physiol. 298 (2010) L744–754, https://doi.org/10.1152/ajplung.00368.2009.

[5] W.L. Lee, A.S. Slutsky, Sepsis and endothelial permeability, N. Engl. J. Med. 363 (2010) 689–691, https://doi.org/10.1056/NEJMcibr1007320.

[6] V. Fanelli, V.M. Ranieri, Mechanisms and clinical consequences of acute lung injury, Ann. Am. Thorac. Soc. 12 (Suppl. 1) (2015) S3–8, https://doi.org/10.1513/AnnalsATS.201407-340MG.

[7] S. Herold, N.M. Gabrielli, I. Vadasz, Novel concepts of acute lung injury and alveolar-capillary barrier dysfunction, Am. J. Physiol. Lung Cell Mol. Physiol. 305 (2013) L665–81, https://doi.org/10.1152/ajplung.00232.2013.

[8] K. Peter, J. Schinnerl, S. Felsinger, L. Brecker, R. Bauer, H. Breiteneder, et al., A novel concept for detoxification: complexation between aconitine and liquiritin in a Chinese herbal formula ('Sini Tang'), J. Ethnopharmacol. 149 (2013) 562–569, https://doi.org/10.1016/j.jep.2013.07.022.

[9] R. Huang, Z. Zhang, M. Xu, X. Chang, Q. Qiao, L. Wang, et al., Effect of Sini decoction on function of hypothalamic-pituitary-adrenal axis in patients with sepsis, Zhonghua wei zhong bing ji jiu yi xue 26 (2014) 184–187, https://doi.org/10.3760/cma.j.issn.2095-4352.2014.03.012.

[10] X. Mujuan, H. Ruolan, C. Xiao, Q. Qiujie, Z. Zhong, W. Ling, The effect of sini decoction on inflammatory cytokines in septic shock patients, Trad. Chin. Med. J. 12 (2013) 43–45, https://doi.org/10.14046/j.cnki.zyytb2002.2013.02.024.

[11] J. Liu, K. Peter, D. Shi, L. Zhang, G. Dong, D. Zhang, et al., Anti-inflammatory effects of the chinese herbal formula sini tang in myocardial infarction rats, Evid. Complement. Alternat. Med. 2014 (2014) 1–10, https://doi.org/10.1155/2014/309378.

[12] F. Lai, G. Zhou, S. Mai, X. Qin, W. Liu, Y. Zhang, et al., Sini decoction improves adrenal function and the short-term outcome of septic rats through downregulation of adrenal toll-like receptor 4 expression, Evid. Based Complement. Altern. Med. 2018 (2018) 9, https://doi.org/10.1155/2018/5186158.

[13] J. Liu, Q. Chen, S. Liu, X. Yang, Y. Zhang, F. Huang, Sini decoction alleviates E. coli induced acute lung injury in mice via equilibrating ACE-AngII-AT1R and ACE2-Ang-(1-7)-Mas axis, Life Sci. (2018) 139–148, https://doi.org/10.1016/j.lfs.2018.07.013.

[14] X.C. Li, D. Zhu, X. Zheng, J. Zhang, J.L. Zhuo, Intratubular and intracellular renin-angiotensin system in the kidney: a unifying perspective in blood pressure control, Clin. Sci. (Lond., Engl.: 1979) 132 (2018) 1383–1401, https://doi.org/10.1042/cs20180121.

[15] C.I. Lin, C.H. Tsai, Y.L. Sun, W.Y. Hsieh, Y.C. Lin, C.Y. Chen, et al., Instillation of particulate matter 2.5 induced acute lung injury and attenuated the injury recovery in ACE2 knockout mice, Int. J. Biol. Sci. 14 (2018) 253–265, https://doi.org/10.7150/ijbs.23489.

[16] W.S.D. Tan, W. Liao, S. Zhou, D. Mei, W.F. Wong, Targeting the renin-angiotensin system as novel therapeutic strategy for pulmonary diseases, Curr. Opin. Pharmacol. 40 (2018) 9–17, https://doi.org/10.1016/j.coph.2017.12.002.

[17] Z. Zou, Y. Yan, Y. Shu, R. Gao, Y. Sun, X. Li, et al., Angiotensin-converting enzyme 2 protects from lethal avian influenza A H5N1 infections, Nat. Commun. 5 (2014) 3594, https://doi.org/10.1038/ncomms4594.

[18] C. Han, J. Liu, X. Liu, M. Li, Angiotensin II induces C-reactive protein expression through ERK1/2 and JNK signaling in human aortic endothelial cells, Atherosclerosis 212 (2010) 206–212, https://doi.org/10.1016/j.atherosclerosis.2010.05.020.

[19] A. Sachse, G. Wolf, Angiotensin II-induced reactive oxygen species and the kidney, J. Am. Soc. Nephrol. 18 (2007) 2439–2446, https://doi.org/10.1681/asn.2007020149.

[20] Y. Li, Y. Cao, Z. Zeng, M. Liang, Y. Xue, C. Xi, et al., Angiotensin-converting enzyme 2/angiotensin-(1-7)/Mas axis prevents lipopolysaccharide-induced apoptosis of pulmonary microvascular endothelial cells by inhibiting JNK/NF-kappaB pathways, Sci. Rep. 5 (2015) 8209, https://doi.org/10.1038/srep08209.

[21] T. Yasuda, MAP kinase cascades in antigen receptor signaling and physiology, Curr. Top. Microbiol. Immunol. 393 (2016) 211–231, https://doi.org/10.1007/82_2015_481.

[22] S. Severin, C. Ghevaert, A. Mazharian, The mitogen-activated protein kinase signaling pathways: role in megakaryocyte differentiation, J. Thromb. Haemost. 8 (2010) 17–26, https://doi.org/10.1111/j.1538-7836.2009.03658.x.

[23] L. Santos, G.B. Rodrigues, F.V.B. Mota, M.E.R. Franca, K.P. de Souza Barbosa, W.H. Oliveira, et al., New thiazolidinedione LPSF/GQ-2 inhibits NFkappaB and MAPK activation in LPS-induced acute lung inflammation, Int. Immunopharmacol. 57 (2018) 91–101, https://doi.org/10.1016/j.intimp.2018.02.011.

[24] D. Zhang, X. Li, Y. Hu, H. Jiang, Y. Wu, Y. Ding, et al., Tabersonine attenuates lipopolysaccharide-induced acute lung injury via suppressing TRAF6 ubiquitination, Biochem. Pharmacol. 154 (2018) 183–192, https://doi.org/10.1016/j.bcp.2018.05.004.

[25] Y. Li, Z. Zeng, Y. Li, W. Huang, M. Zhou, X. Zhang, et al., Angiotensin-converting enzyme inhibition attenuates lipopolysaccharide-induced lung injury by regulating the balance between angiotensin-converting enzyme and angiotensin-converting enzyme 2 and inhibiting mitogen-activated protein kinase activation, Shock 43 (2015) 395–404, https://doi.org/10.1097/shk.0000000000000302.

[26] Meng YingMeng, Yu ChangHuiYu, Li WeiLi, et al., Angiotensin-Converting Enzyme 2/Angiotensin-(1-7)/Mas Axis Protects against Lung Fibrosis by Inhibiting the MAPK/NF-κB Pathway, Am. J. Respir. Cell Mol. Biol. 50 (2014) 723–736.

[27] S.F. Luo, R.Y. Fang, H.L. Hsieh, P.L. Chi, C. Lin, L.D. Hsiao, et al., Involvement of MAPKs and NF-kappaB in tumor necrosis factor alpha-induced vascular cell adhesion molecule 1 expression in human rheumatoid arthritis synovial fibroblasts, Arthritis Rheum. 62 (2010) 105–116, https://doi.org/10.1002/art.25060.

[28] K. Xie, Y. Yu, Y. Huang, L. Zheng, J. Li, H. Chen, et al., Molecular hydrogen ameliorates lipopolysaccharide-induced acute lung injury in mice through reducing inflammation and apoptosis, Shock 37 (2012) 548, https://doi.org/10.1097/SHK.0b013e31824ddc81.

[29] W. Wei, L. Dejie, S. Xiaojing, W. Tiancheng, C. Yongguo, Y. Zhengtao, et al., Magnolol inhibits the inflammatory response in mouse mammary epithelial cells and a mouse mastitis model, Inflammation 38 (2015) 16–26, https://doi.org/10.1007/s10753-014-0003-2.

[30] Z.J. Ma, L. Lu, J. Yang, X. Wang, G. Su, Z.L. Wang, et al., Lariciresinol induces apoptosis in HepG2 cells via mitochondrial-mediated apoptosis pathway, Eur. J. Pharmacol. 821 (2018) 1–10, https://doi.org/10.1016/j.ejphar.2017.12.027.

[31] K.N. Iskander, M.F. Osuchowski, D.J. Stearns-Kurosawa, S. Kurosawa, D. Stepien, C. Valentine, et al., Sepsis: multiple abnormalities, heterogeneous responses, and evolving understanding, Physiol. Rev. 93 (2013) 1247–1288, https://doi.org/10.1152/physrev.00037.2012.

[32] L. Pedrazza, M. Cubillos-Rojas, F. de Mesquita, C. Luft, A. Cunha, J. Rosa, et al., Mesenchymal stem cells decrease lung inflammation during sepsis, acting through inhibition of the MAPK pathway, Stem Cell Res. Ther. 8 (2017) 289, https://doi.org/10.1186/s13287-017-0734-8.

[33] M.R. Passmore, L. Byrne, N.G. Obonyo, L.E. See Hoe, A.C. Boon, S.D. Diab, et al., Inflammation and lung injury in an ovine model of fluid resuscitated endotoxemic shock, Respir. Res. 19 (2018) 231, https://doi.org/10.1186/s12931-018-0935-4.

[34] A. Haegens, P. Heeringa, R.J. van Suylen, C. Steele, Y. Aratani, R.J. O'Donoghue, et al., Myeloperoxidase deficiency attenuates lipopolysaccharide-induced acute lung inflammation and subsequent cytokine and chemokine production, J. Immunol. (Baltimore, Md.: 1950) 182 (2009) 7990–7996, https://doi.org/10.4049/jimmunol.0800377.

[35] J. Guo, H. Huo, L. Li, S. Guo, T. Jiang, Sini tang prevents depression-like behavior in rats exposed to chronic unpredictable stress, Am. J. Chin. Med. 37 (2009) 261–272, https://doi.org/10.1142/S0192415X0900693X.

[36] M.A. Matthay, L.B. Ware, G.A. Zimmerman, The acute respiratory distress syndrome, J. Clin. Invest. 122 (2012) 2731–2740, https://doi.org/10.1172/jci60331.

[37] Q. Zhang, D. Wu, Y. Yang, T. Liu, H. Liu, Dexmedetomidine alleviates hyperoxia-induced acute lung injury via inhibiting NLRP3 inflammasome activation, Cell. Physiol. Biochem. Int. J. Exp. Cell. Physiol. Biochem. Pharmacol. 42 (2017) 1907, https://doi.org/10.1159/000479609.

[38] S.E. Tang, C.P. Wu, S.Y. Wu, C.K. Peng, W.C. Perng, B.H. Kang, et al., Stanniocalcin-1 ameliorates lipopolysaccharide-induced pulmonary oxidative stress, inflammation, and apoptosis in mice, Free Radic. Biol. Med. 71 (2014) 321–331, https://doi.org/10.1016/j.freeradbiomed.2014.03.034.

[39] A.J. Turner, N.M. Hooper, The angiotensin-converting enzyme gene family: genomics and pharmacology, Trends Pharmacol. Sci. 23 (2002) 177–183.

[40] J. Zhong, R. Basu, D. Guo, F.L. Chow, S. Byrns, M. Schuster, et al., Angiotensin-converting enzyme 2 suppresses pathological hypertrophy, myocardial fibrosis, and cardiac dysfunction, Circulation 122 (717-28) (2010) 18, https://doi.org/10.1161/circulationaha.110.955369 following 28.

[41] L. Tao, Y. Qiu, X. Fu, R. Lin, C. Lei, J. Wang, et al., Angiotensin-converting enzyme 2 activator diminazene aceturate prevents lipopolysaccharide-induced inflammation

by inhibiting MAPK and NF-κB pathways in human retinal pigment epithelium, J. Neuroinflammation 13 (2016) 35.

[42] H. Bao, F. Gao, G. Xie, Z. Liu, Angiotensin-converting enzyme 2 inhibits apoptosis of pulmonary endothelial cells during acute lung injury through suppressing MiR-4262, Cell. Physiol. Biochem. 37 (2015) 759–767, https://doi.org/10.1159/000374025.

[43] S. Chan, Y. Lau, A. Miller, J. Ku, S. Potocnik, J. Ye, et al., Angiotensin II causes β-cell dysfunction through an ER stress-induced proinflammatory response, Endocrinology 158 (2017) 3162–3173.

[44] K.D. da Silveira, F.M. Coelho, A.T. Vieira, D. Sachs, L.C. Barroso, V. Costa, et al., Anti-inflammatory effects of the activation of the angiotensin-(1-7) receptor, MAS, in experimental models of arthritis, J. Immunol. (Baltimore, Md. : 1950) 185 (2010) 5569–5576, https://doi.org/10.4049/jimmunol.1000314.

[45] P.J. Barnes, M. Karin, Nuclear factor-kappaB: a pivotal transcription factor in chronic inflammatory diseases, N. Engl. J. Med. 336 (1997) 1066–1071, https://doi.org/10.1056/nejm199704103361506.

[46] S.R. Kim, H.J. Kim, D.I. Kim, K.B. Lee, H.J. Park, J.S. Jeong, et al., Blockade of interplay between IL-17A and endoplasmic reticulum stress attenuates LPS-Induced lung injury, Theranostics 5 (2015) 1343–1362, https://doi.org/10.7150/thno.11685.

[47] J.H. Lee, D.S. Min, C.W. Lee, K.H. Song, Y.S. Kim, H.P. Kim, Ginsenosides from Korean Red Ginseng ameliorate lung inflammatory responses: inhibition of the MAPKs/NF-kappaB/c-Fos pathways, J. Ginseng Res. 42 (2018) 476–484, https://doi.org/10.1016/j.jgr.2017.05.005.